Available online at www.sciencedirect.com
ScienceDirect
International Journal of Solids and Structures 43 (2006) 6052–6070
INTERNATIONAL JOURNAL OF SOLIDS and STRUCTURES
www.elsevier.com/locate/ijsolstr

A polyconvex framework for soft biological tissues. Adjustment to experimental data

D. Balzani [a,*], P. Neff [b], J. Schröder [c], G.A. Holzapfel [d]

[a] *Fachbereich Mechanik (AG4), Technische Universität Darmstadt, Hochschulstr. 1, 64289 Darmstadt, Germany*
[b] *Fachbereich Mathematik, Technische Universität Darmstadt, Schloßgartenstr. 7, 64289 Darmstadt, Germany*
[c] *Institut für Mechanik, Fachbereich 10, Universität Duisburg-Essen, Standort Essen, Universitätsstr. 15, 45117 Essen, Germany*
[d] *School of Engineering Sciences, Royal Institute of Technology (KTH), Osquars backe 1, SE-100 44 Stockholm, Sweden*

Received 22 May 2005
Available online 19 September 2005

Abstract

The main goal of this contribution is to provide a simple method for constructing transversely isotropic polyconvex functions suitable for the description of biological soft tissues. The advantage of our approach is that only a few parameters are necessary to approximate a variety of stress–strain curves and to satisfy the condition of a stress-free reference configuration a priori in the framework of polyconvexity. The proposed polyconvex stored energies are embedded into the concept of structural tensors and the representation theorems for isotropic tensor functions are utilized. As an example, the medial layer of a human abdominal aorta is investigated, modeled by some of the proposed polyconvex functions and compared with experimental data. Hereby, the economic fitting to experimental data, and hence the easy handling of the functions is shown.

Keywords: Anisotropic; Polyconvex; Hyperelastic; Stored energy function; Biological soft tissues

1. Introduction

The understanding of living matter as a mechanical system requires appropriate mechanical tests and related efficient constitutive models. Several types of, e.g., soft biological tissues are frequently characterized as fiber–reinforced composites, and the basic idea is to formulate constitutive models which incorporate some histological information, i.e. the non-collagenous matrix, collagen fibers among others. The collagen fibers,

* Corresponding author.
E-mail address: balzani@mechanik.tu-darmstadt.de (D. Balzani).

0020-7683/$ - see front matter
doi:10.1016/j.ijsolstr.2005.07.048

e.g., induce the anisotropy in the mechanical response such that the overall response of arterial tissue is orthotropic and is accounted for by the constitutive theory of fiber–reinforced solids. The anisotropy can be represented via the introduction of a so-called structural tensor, which allows a coordinate-invariant formulation of the constitutive equations. For an introduction to the concept of structural tensors, also denoted as the concept of integrity bases, used for the construction of isotropic and anisotropic tensor functions, see, e.g., Spencer (1971), Boehler (1987), Betten (1987) and Zheng and Spencer (1993a,b).

In the framework of computer simulations with Newton type methods the mathematical treatment of the underlying boundary-value problems is based on the direct methods of the calculus of variations. In this context the constitutive equations, represented by the stored-energy function, have not only to be able to reflect the material properties, but should satisfy some generalized convexity conditions, too, in order to obtain a physically reasonable and numerically stable material model.

The existence of minimizers of some variational principles in finite elasticity is based on the concept of quasiconvexity, introduced by Morrey (1952). This inequality condition is rather complicated to handle since it is an integral inequality. Thus, a more important concept for practical use is the notion of polyconvexity in the sense of Ball (1977a,b), in this context see also Marsden and Hughes (1983) and Ciarlet (1988). For isotropic material response functions there exist some well-known models, e.g., the Ogden-, Mooney–Rivlin- and Neo–Hooke-type models, which fall into this concept. It should be noted, that for isotropic polyconvex functions of the Mooney–Rivlin-type a minimum number of four material parameters is necessary in order to recover the classical Lamé constants of linear elasticity λ and μ, and to satisfy the condition of a stress-free reference configuration, see Ciarlet (1988). For the application of the framework of polyconvexity to nearly incompressible isotropic hyperelasticity see, e.g., Hartmann and Neff (2003), where also the coercivity question is treated. We note that quasiconvexity together with coercivity is sufficient for the existence of minimizers and that coercivity is practically only a condition on the isotropic part of the stored energy. The extension of polyconvexity to anisotropy has been first given in Schröder and Neff (2001). In Schröder and Neff (2003) the proof of polyconvexity of a variety of isotropic and transversely isotropic functions is given. A polyconvex model, which is constructed in the abstract framework of these functions, is proposed in Itskov and Aksel (2004) for the description of calendered rubber sheets showing a marked anisotropy. The extension to polyconvex anisotropic stored-energy functions in terms of the right symmetric stretch tensor is worked out in Steigmann (2003). It can be shown that polyconvexity of the stored energy implies that the corresponding acoustic tensor is elliptic for all deformations, which means from the physical point of view that only real wave speeds occur; then the material is said to be stable. For an illustration of this implication in Schröder et al. (2004) a localization analysis is performed comparatively for non-polyconvex functions and a polyconvex one. Therein it is shown that no problems with respect to material stability occur when the polyconvex model is utilized. Note that the precise difference between the local property of ellipticity and the non-local condition of quasiconvexity is still an active topic for research.

For stress analysis in biomechanics exponential-type laws are often used, see, e.g., Almeida and Spilker (1998), Fung et al. (1979), Humphrey (2002), and the references therein. In Schröder et al. (2004) a polyconvex model including the quadratic terms in the right Cauchy–Green tensor is adjusted to the media and adventitia of an artery of a rabbit. A drawback of the two models in Schröder et al. (2004) and Itskov and Aksel (2004) is the large number of material parameters necessary to represent the material behavior. A materially stable constitutive model for the simulation of arterial walls has been developed in Holzapfel et al. (2000) (with extensions to the inelastic domain Gasser and Holzapfel, 2002; Holzapfel et al., 2002), where each layer of the artery is modeled as a fiber–reinforced material. In this model the convexity of the transversely isotropic part can be obtained by an appropriate case distinction switching the function off in the non-convex range. This idea of a switch motivates us to extend it to other polyconvex functions with possibly less material parameters. This is the main effort of this work, to construct polyconvex functions with less material parameters, which can easily be handled and which are able to represent the basic characteristics of soft biological tissues.

This paper is organized as follows: in Section 2 we briefly review some terminology in non-linear continuum mechanics. Section 3 gives an insight into the concept of structural tensors and the representation theorems for isotropic tensor functions. In Section 4 generalized convexity conditions, especially the polyconvexity condition, are recapitulated. Furthermore, a simple construction principle for polyconvex functions and the proposed polyconvex stored energies governed by this principle are given. In Section 5 experimental data of the medial layer of a human abdominal aorta is represented by a set of proposed polyconvex functions, in order to show its practical utility. Section 6 summarizes the results.

2. Continuum mechanical foundation

The body of interest in the reference configuration is denoted by $\mathscr{B} \subset \mathbb{R}^3$, parametrized in $\boldsymbol{X}$, and the current configuration by $\mathscr{S} \subset \mathbb{R}^3$, parametrized in $\boldsymbol{x}$. The non-linear deformation map $\boldsymbol{\varphi}_t : \mathscr{B} \to \mathscr{S}$ at time $t \in \mathbb{R}_+$ maps points $\boldsymbol{X} \in \mathscr{B}$ onto points $\boldsymbol{x} \in \mathscr{S}$. The deformation gradient $\boldsymbol{F}$ is defined by

$$\boldsymbol{F}(\boldsymbol{X}) := \nabla \boldsymbol{\varphi}_t(\boldsymbol{X}) \tag{2.1}$$

with the Jacobian $J(\boldsymbol{X}) := \det \boldsymbol{F}(\boldsymbol{X}) > 0$. The index notation of $\boldsymbol{F}$ is $F^a_{\ A} := \partial x^a / \partial X^A$. The right Cauchy–Green tensor is defined by

$$\boldsymbol{C} := \boldsymbol{F}^{\mathrm{T}} \boldsymbol{F} \quad \text{with} \quad C_{AB} = F^a_{\ A} F^b_{\ B} g_{ab}, \tag{2.2}$$

where $\boldsymbol{g}$ denotes the covariant metric tensor in the current configuration. The standard covariant metric tensors $\boldsymbol{G}$ and $\boldsymbol{g}$ within the Lagrange and Eulerian settings appear in the index representation G_{AB} and g_{ab}, respectively. Thus the contravariant metric tensors $\boldsymbol{G}^{-1}$ and $\boldsymbol{g}^{-1}$ have the index representation G^{AB} and g^{ab}, respectively. For the representations in Cartesian coordinates we arrive at the simple expressions $G_{AB} = G^{AB} = \delta_{AB}$ for Lagrangian metric tensors and $g_{ab} = g^{ab} = \delta_{ab}$ for the Eulerian metric tensors. For the geometrical interpretations of the polynomial invariants in the following sections we often use expressions based on the mappings of the infinitesimal line $\mathrm{d}\boldsymbol{X}$, area $\mathrm{d}\boldsymbol{A} = \boldsymbol{N}\mathrm{d}A$ and volume elements $\mathrm{d}V$. These material quantities are mapped to their spatial counterparts $\mathrm{d}\boldsymbol{x}$, $\mathrm{d}\boldsymbol{a} = \boldsymbol{n}\,\mathrm{da}$ and $\mathrm{d}v$ via

$$\mathrm{d}\boldsymbol{x} = \boldsymbol{F}\,\mathrm{d}\boldsymbol{X}, \quad \boldsymbol{n}\,\mathrm{d}a = \mathrm{Cof}[\boldsymbol{F}]\boldsymbol{N}\,\mathrm{d}A \quad \text{and} \quad \mathrm{d}v = \det[\boldsymbol{F}]\,\mathrm{d}V. \tag{2.3}$$

Eq. $(2.3)_2$ is the well-known Nanson's formula. It should be mentioned that the argument $(\boldsymbol{F}, \mathrm{Adj}\boldsymbol{F}, \det\boldsymbol{F})$, with $\mathrm{Adj}\boldsymbol{F} = (\mathrm{Cof}\boldsymbol{F})^{\mathrm{T}}$, plays an important role in the definition of polyconvexity; this will be discussed in detail in Section 4.

We consider hyperelastic materials which postulate the existence of a so-called stored-energy function ψ, defined per unit reference volume. Reduced constitutive equations which satisfy a priori the principle of material objectivity yield, e.g., the functional dependence $\psi = \hat{\psi}(\boldsymbol{C})$, see e.g., Truesdell and Noll (2004). If we assume the stored-energy function to be a function of the right Cauchy–Green tensor, i.e. $\hat{\psi}(\boldsymbol{C})$, we obtain the second Piola–Kirchhoff stresses

$$\boldsymbol{S} = 2\partial_C \hat{\psi}(\boldsymbol{C}). \tag{2.4}$$

The first Piola–Kirchhoff stress tensor, which plays an essential role in generalized convexity conditions is given by $\boldsymbol{P} = \boldsymbol{F}\boldsymbol{S}$. The (real) Cauchy stresses can be calculated by the transformation $\boldsymbol{\sigma} = \det[\boldsymbol{F}]^{-1}\boldsymbol{F}\boldsymbol{S}\boldsymbol{F}^{\mathrm{T}}$.

An important concept for the description of anisotropic materials is the principle of material symmetry. Let us introduce a material symmetry group $\mathscr{G}_k$ with respect to a local reference configuration, which characterizes the anisotropy class of the material. The elements of $\mathscr{G}_k$ are denoted by the unimodular tensors ${}^i\boldsymbol{Q} | i = 1, \ldots, n$. The concept of material symmetry requires the constitutive equations to be invariant under transformations with elements of the symmetry group, i.e.

$$\hat{\psi}(\boldsymbol{F}\boldsymbol{Q}) = \hat{\psi}(\boldsymbol{F}) \quad \forall \boldsymbol{Q} \in \mathscr{G}_k, \boldsymbol{F}. \tag{2.5}$$

Thus, superimposed rotations and reflections on the reference configuration with elements of the material symmetry group do not influence the behavior of the anisotropic material. The symmetries impose several restrictions on the form of the constitutive functions. In order to work out the explicit restrictions for the individual symmetry groups, or more reasonably to point out general forms of the functions which satisfy these restrictions, it is necessary to use representation theorems for anisotropic tensor functions. This allows us to formulate the stored-energy function as an isotropic tensor function with respect to an extended tensorial argument list.

3. Coordinate-invariant formulation

The main idea is the extension of $\mathscr{G}_k$-invariant functions (2.5) into functions which are invariant under a larger group, here the special orthogonal group. This implies that it is in principle possible to transform an anisotropic constitutive function into an isotropic one through certain tensors called structural tensors, which reflect the symmetry group of the considered material. The concept of structural tensors was first introduced in an attractive way with important applications by Boehler in 1978–1979, although some similar ideas might have been formulated earlier. Here we only consider anisotropic materials which can be characterized by certain directions. That means that the anisotropy can be described by some unit vectors $\boldsymbol{a}_{(a)}$ and some second-order tensors $\boldsymbol{M}_{(a)}$ defined in the reference configuration, in this context we refer to Zheng and Boehler (1994). In the sequel, we restrict ourselves to the cases of transverse isotropy and to materials which can be characterized by two non-orthogonal preferred directions. In these cases we are able to express the material symmetry of the considered body by a set of second-order structural tensors. Let $\mathscr{G}_M$ be the invariance group of the structural tensors, i.e.

$$\mathscr{G}_M := \{\boldsymbol{Q} \in \mathrm{SO}(3), \boldsymbol{Q} * \boldsymbol{\xi} = \boldsymbol{\xi}\} \tag{3.6}$$

with $\boldsymbol{\xi} := \{\boldsymbol{M}_{(a)}\}$ and $a = 1$ for transversely isotropic and $a = 1, 2$ for the second class. The transformations ${}^{i}\boldsymbol{Q} | i = 1, \ldots, n$ represent rotations and reflections with respect to preferred directions and planes. In the sequel, we skip the index $(\bullet)_{(a)}$ if there is no danger of confusion. The last term in (3.6) characterizes the mapping $\boldsymbol{\xi} \rightarrow \boldsymbol{Q} * \boldsymbol{\xi} := \{\boldsymbol{Q}^{\mathrm{T}}\boldsymbol{M}\boldsymbol{Q}\}$. If $\mathscr{G}_M \equiv \mathscr{G}_K$, where $\mathscr{G}_K$ is defined by (2.5), then the invariance group preserves the characteristics of the anisotropic solid. Let us now assume the existence of a set of $\mathscr{G}_k$-invariant structural tensors $\boldsymbol{\xi}$. Now we can transform (2.5) into a function which is invariant under the special orthogonal group. This leads to a scalar-valued isotropic tensor function in an extended argument list. That means from the mechanical point of view that rotations superimposed onto the reference configuration with the mappings $\boldsymbol{X} \rightarrow \boldsymbol{Q}^{\mathrm{T}}\boldsymbol{X}$ and $\boldsymbol{\xi} \rightarrow \boldsymbol{Q} * \boldsymbol{\xi}$ for arbitrary rotations lead to the condition $\psi = \hat{\psi}(\boldsymbol{F}, \boldsymbol{\xi}) = \hat{\psi}(\boldsymbol{F}\boldsymbol{Q}, \boldsymbol{Q} * \boldsymbol{\xi})$ $\forall \boldsymbol{Q} \in \mathrm{SO}(3)$. Due to the concept of material frame indifference we arrive at a further reduction of the constitutive equation of the form

$$\psi = \hat{\psi}(\boldsymbol{C}, \boldsymbol{\xi}) = \hat{\psi}(\boldsymbol{Q}^{\mathrm{T}}\boldsymbol{C}\boldsymbol{Q}, \boldsymbol{Q} * \boldsymbol{\xi}) \quad \forall \boldsymbol{Q} \in \mathrm{SO}(3), \tag{3.7}$$

which is the definition of an isotropic scalar-valued tensor function in the arguments $(\boldsymbol{C}, \boldsymbol{\xi})$.

For the construction of specific constitutive equations the invariants of the deformation tensor and of the additional structural tensor are necessary. An irreducible polynomial basis consists of a collection of members, where none of them can be expressed as a polynomial function of the others. Based on the Hilbert theorem, cf. Gurevich (1964), there exists for a finite basis of tensors a finite integrity basis. Transverse isotropy is characterized by one preferred unit direction $\boldsymbol{a}$ and the material symmetry group is defined by

$$\mathscr{G}_{\mathrm{ti}} := \{\boldsymbol{I}; \boldsymbol{Q}(\alpha, \boldsymbol{a}) | 0 < \alpha < 2\pi\}, \tag{3.8}$$

where $\boldsymbol{Q}(\alpha, \boldsymbol{a})$ are all rotations about the $\boldsymbol{a}$-axis. The structural tensor $\boldsymbol{M}$ whose invariance group preserves the material symmetry group $\mathscr{G}_{\text{ti}}$ is given by

$$\boldsymbol{M} := \boldsymbol{a} \otimes \boldsymbol{a}. \tag{3.9}$$

The integrity basis consists of the traces of products of powers of the argument tensors, the so-called principal invariants and the mixed invariants. The principal invariants $I_k = \hat{I}_k(\boldsymbol{C}),\ k = 1, 2, 3$ of a second-order tensor $\boldsymbol{C}$ are defined as the coefficients of the characteristic polynomial

$$f(\lambda) = \det[\lambda \mathbf{1} - \boldsymbol{C}] = \sum_{k=0}^{3} (-1)^k I_k \lambda^{n-k}, \tag{3.10}$$

with $I_0 = 1$. The explicit expressions for the principle invariants of the considered second-order tensor are given by

$$I_1 := \operatorname{tr}\boldsymbol{C}, \quad I_2 := \operatorname{tr}[\operatorname{Cof}\boldsymbol{C}], \quad I_3 := \det \boldsymbol{C}. \tag{3.11}$$

These invariants can also be expressed in terms of the so-called basic invariants J_i, $i = 1, 2, 3$. They are defined by the traces of powers of $\boldsymbol{C}$, i.e.

$$J_1 := \operatorname{tr}\boldsymbol{C}, \quad J_2 := \operatorname{tr}[\boldsymbol{C}^2], \quad J_3 := \operatorname{tr}[\boldsymbol{C}^3]. \tag{3.12}$$

These quantities are related to the principal invariants by the simple algebraic expressions

$$J_1 := I_1, \quad J_2 := I_1^2 - 2I_2, \quad J_3 := I_1^3 - 3I_1 I_2 + 3I_3. \tag{3.13}$$

Let $\boldsymbol{M}$ be of rank one and let us assume the normalization condition $\|\boldsymbol{M}\| = 1$, then the additional invariants, the so-called mixed invariants, are

$$J_4 := \operatorname{tr}[\boldsymbol{C}\boldsymbol{M}], \quad J_5 := \operatorname{tr}[\boldsymbol{C}^2\boldsymbol{M}], \tag{3.14}$$

see, e.g., Spencer (1987) and the references therein. For the construction of constitutive equations it is necessary to determine the minimal set of invariants from which all other invariants can be generated. Here we focus on polynomial invariants. The integrity basis is defined by the set of polynomial invariants which allows the construction of any polynomial invariant as a polynomial in members of the given set, see, e.g., Spencer (1971). The polynomial basis for the construction of a specific stored-energy function ψ is given by

$$\mathscr{P}_1 := \{I_1, I_2, I_3, J_4, J_5\} \quad \text{or} \quad \mathscr{P}_2 := \{J_1, \ldots, J_5\}. \tag{3.15}$$

The bases (3.15) are invariant under all transformations with elements of $\mathscr{G}_{\text{ti}}$. As a result the polynomial functions in elements of the polynomial basis are also invariant under these transformations. For the stored-energy function we assume the general form

$$\psi = \hat{\psi}(L_i | L_i \in \mathscr{P}_j) + c \quad \text{for } j = 1 \text{ or } j = 2. \tag{3.16}$$

In order to satisfy the non-essential normalization condition $\psi(\mathbf{1}) = 0$ we have introduced the constant $c \in \mathbb{R}$.

4. Polyconvex stored-energy functions

4.1. Generalized convexity conditions

A very important semiconvexity condition is proposed by Morrey (1952): the quasiconvexity. This integral inequality condition implies that the state of minimum energy for a homogeneous body under homogeneous Dirichlet boundary conditions is itself homogeneous. If the stored energy is not quasiconvex, the

initially homogeneous material body could break down in coexisting stable phases, see Krawietz (1986), Ball and James (1992), Silhavý (1997), Müller (1999), and the references therein. Furthermore, the quasiconvexity inequality together with coercivity represents the sufficient condition for the existence of minimizers. Since the quasiconvexity condition is an integral inequality and, therefore, a non-local condition, it is rather complicated to check. A local, and hence a more tractable concept is the notion of polyconvexity in the sense of Ball (1977a,b). For finite-valued, continuous functions we may recapitulate the important implications, that polyconvexity implies quasiconvexity and this implies rank-one convexity. The converse implications are not true, see, e.g., Dacorogna (1989) and Silhavý (1997). Considering smooth stored-energy functions the (strict) rank-one convexity implies the (strict) Legendre–Hadamard condition. This is a suitable condition in order to obtain physically reasonable material models, because hereby, the existence of real wave speeds are guaranteed. In this context see also Schröder et al. (2004). Recapitulating, a smooth polyconvex stored-energy function ensures automatically the fulfillment of the quasiconvexity-, the rank-one convexity- and the Legendre–Hadamard condition, without obtaining the physical drawbacks of the convexity condition.

Polyconvexity: $\boldsymbol{F} \mapsto W(\boldsymbol{F})$ is polyconvex if and only if there exists a function $P : \mathbb{R}^{3\times3} \times \mathbb{R}^{3\times3} \times \mathbb{R} \mapsto \mathbb{R}$ (in general non-unique) such that

$$W(\boldsymbol{F}) = P(\boldsymbol{F}, \mathrm{Adj}[\boldsymbol{F}], \det[\boldsymbol{F}])$$

and the function $\mathbb{R}^{19}\mapsto\mathbb{R}$, $(\boldsymbol{F}, \mathrm{Adj}[\boldsymbol{F}], \det[\boldsymbol{F}]) \mapsto P(\boldsymbol{F}, \mathrm{Adj}[\boldsymbol{F}], \det[\boldsymbol{F}])$ is convex for all points $\boldsymbol{X} \in \mathbb{R}^3$.

In the above definition and in the sequel we omit the $\boldsymbol{X}$-dependence of the individual functions if there is no danger of confusion. The adjugate of $\boldsymbol{F}$ is defined by $\mathrm{Adj}[\boldsymbol{F}] = \det[\boldsymbol{F}]\boldsymbol{F}^{-1}$ for all invertible $\boldsymbol{F}$.

4.2. Stored-energy function for soft biological tissues

Generally, from the mechanical point of view, soft biological tissues may be characterized as an isotropic non-collagenous matrix, the so-called ground substance, in which collagen fibers are embedded. While in, e.g., ligaments or tendons the fibers are arranged mainly in one direction, the fibers in, e.g., arterial walls are considered to be oriented in two directions helically wound along the arterial axis and symmetrically disposed with respect to the axis. In this case the material behavior in fiber direction can be represented by the superposition of two transversely isotropic models (for arguments see Holzapfel et al., 2000), and we obtain for the general case a stored energy of the form

$$\psi = \psi^{\mathrm{iso}} + \sum_{a=1}^{n} \psi^{\mathrm{ti},(a)}.$$

Herein, $\psi^{\mathrm{ti},(a)}$ denotes the transversely isotropic stored energy for one fiber family characterized by $\boldsymbol{a}_{(a)}$. Note that for tissues as, e.g., ligaments or tendons we set $n = 1$ and for, e.g., arterial walls $n = 2$. Since the fibers themselves do not differ with their orientation, the material parameters in $\psi^{\mathrm{ti},(a)}$ remain unaltered for all fiber directions.

4.2.1. Isotropic polyconvex functions

Since we assume the ground substance in soft tissues to behave in an isotropic manner we require isotropic functions for its description. One function, which satisfies the stress-free reference configuration a priori, is given as

$$\psi^{\mathrm{iso}}_{(\mathrm{P1})} = c_1 \left(\frac{I_1}{I_3^{1/3}} - 3 \right), \quad c_1 > 0, \tag{4.17}$$

and similarly used in Weiss et al. (1996) and also in Holzapfel et al. (2000, 2004a). Another function for the isotropic part of soft biological tissues is

$$\psi^{\text{iso}}_{(\text{P2})} = c_2\left(\frac{I_2}{I_3^{1/3}} - 3\right), \quad c_2 > 0. \tag{4.18}$$

The difference between the latter two functions is the usage of I_1 and I_2 and therewith the use of terms in $\boldsymbol{C}$ and in $\text{Cof}\boldsymbol{C}$, respectively. In the present work we are interested in satisfying the quasi-incompressibility constraint not by special FE-approaches; thus, we need a function that penalizes volumetric deformations. A suitable function for this purpose is given by

$$\psi^{\text{iso}}_{(\text{P3})} = \varepsilon\left(I_3^{\gamma} + \frac{1}{I_3^{\gamma}} - 2\right), \quad \varepsilon > 0, \;\; \gamma > 1. \tag{4.19}$$

It is worth noting that all functions given in this section are polyconvex and lead to stresses which are zero in the reference configuration.

4.2.2. Transversely isotropic polyconvex functions

Soft biological tissues are characterized by an exponential-type stress–strain behavior in the fiber direction. A model for the description of these materials, which also satisfies the stress-free reference configuration, is proposed by Holzapfel et al. (2004a) (firstly in Holzapfel et al., 2000). The transversely isotropic function appears as

$$\psi^{\text{ti},(a)}_{(\text{HGO})} = \begin{cases} \frac{k_1}{2k_2}\{\exp[k_2(J_4^{(a)} - 1)^2] - 1\} & \text{for } J_4^{(a)} \geqslant 1, \\ 0 & \text{for } J_4^{(a)} < 1, \end{cases} \tag{4.20}$$

where $k_1 \geqslant 0$ is a stress-like material parameter and $k_2 > 0$ is a dimensionless parameter. An appropriate choice of k_1 and k_2 enables the histologically-based assumption that the collagen fibers do not influence the mechanical response of the artery in the low pressure domain to be modeled (Roach and Burton, 1957). The proof of convexity of (4.20) with respect to $\boldsymbol{F}$ is, e.g., given in Schröder et al. (2004), see also Appendix A. Due to the fact that $J_4^{(a)}$ represents the square of the stretch in fiber direction $\boldsymbol{a}_{(a)}$ the distinction of cases in (4.20) seems to be reasonable, because $J_4^{(a)} < 1$ characterizes the shortening of the fibers, which is assumed to generate no stresses. Note that replacing $J_4^{(a)}$ by its isochoric part $\overline{J}_4^{(a)} = J_4^{(a)}/I_3^{1/3}$ leaves (4.20) polyconvex provided that the case-distinction is adapted accordingly.

The structure of (4.20) motivates the construction of another convex stored-energy function of the form

$$\psi^{\text{ti},(a)}_{(\text{P1})} = \begin{cases} \alpha_1(J_4^{(a)} - 1)^{\alpha_2} & \text{for } J_4^{(a)} \geqslant 1, \\ 0 & \text{for } J_4^{(a)} < 1 \end{cases} \tag{4.21}$$

with $\alpha_1 \geqslant 0$ and $\alpha_2 > 1$. In Schröder and Neff (2003), Corollary B.7, it has been observed that if a function $P : \mathbb{R}^n \mapsto \mathbb{R}$ is convex and $P(Z) \geqslant 0$, then the function $Z \in \mathbb{R}^n \mapsto [P(Z)]^p$ is also convex for $p \geqslant 1$. Since $(J_4^{(a)} - 1)$ is convex and positive for $J_4^{(a)} \geqslant 1$ the convexity of (4.21) is obvious; for the complete proof of convexity see Appendix A. Note that the replacement of $J_4^{(a)}$ by its isochoric part $\overline{J}_4^{(a)}$ is also possible without violating the convexity condition. Additionally note that the natural state condition is satisfied.

As it has been observed more generally in Schröder and Neff (2003), Lemma B.9, a function $\mathbb{R}^n \mapsto \mathbb{R}$, $X \mapsto m(P(X))$ is convex, if the function $P : \mathbb{R}^n \mapsto \mathbb{R}$ is convex and the function $m : \mathbb{R} \mapsto \mathbb{R}$ is convex and monotonically increasing. Reconsidering the last two stored-energy functions we notice that the functions fit into the latter structure, i.e. $\exp[\cdots]$ is monotonically increasing and convex and $(\cdots)^p$ is convex and monotonically increasing for positive arguments. This motivates the replacement of $J_4^{(a)}$ in (4.20) and (4.21) by an arbitrary polyconvex function provided that the case-distinction is adapted accordingly. For this purpose the transversely isotropic functions already given in Schröder and Neff (2003)

$$(J_4^{(a)})^2, \quad \frac{J_4^{(a)}}{I_3^{1/3}}, \quad \frac{(J_4^{(a)})^2}{I_3^{1/3}}, \quad (K_2^{(a)})^2, \quad \frac{K_2^{(a)}}{I_3^{1/3}}, \quad \frac{(K_2^{(a)})^2}{I_3^{2/3}} \tag{4.22}$$

(recall that $K_2^{(a)} := \mathrm{tr}[\boldsymbol{C}\boldsymbol{D}_{(a)}]$ with $\boldsymbol{D}_{(a)} = \boldsymbol{1} - \boldsymbol{M}_{(a)}$) may be used. The construction principle for polyconvex functions which also satisfy the stress-free reference configuration can then be rephrased in words as the following problem:

find an (inner) polyconvex function $P(X)$ which is zero in the reference configuration and include this function into any arbitrary convex and monotonically increasing function m by setting $m = m(P(X))$,

cf. Schröder and Neff (2003), Lemma B.9. Due to the fact that the functions given in (4.20) and (4.21) are linear in $\boldsymbol{C}$ and possess, therefore, a relatively limited mapping range, the supply of quadratic terms in $\boldsymbol{C}$ seems to be profitable. The probably most straightforward method is the substitution of $J_4^{(a)}$ by $J_5^{(a)}$ in (4.20) or (4.21), but unfortunately such functions will not be polyconvex; cf. Merodio and Neff (submitted for publication). In Schröder and Neff (2003) the two polyconvex functions

$$K_1^{(a)} := \mathrm{tr}[\mathrm{Cof}[\boldsymbol{C}]\boldsymbol{M}_{(a)}] \quad \text{and} \quad K_3^{(a)} := \mathrm{tr}[\mathrm{Cof}[\boldsymbol{C}]\boldsymbol{D}_{(a)}] \tag{4.23}$$

(with $\boldsymbol{D}_{(a)} := \boldsymbol{1} - \boldsymbol{M}_{(a)}$), which are quadratic in $\boldsymbol{C}$, are given and their polyconvexity is shown (recall that $K_1^{(a)} = J_5^{(a)} - I_1 J_4^{(a)} + I_2$ and $K_3^{(a)} = I_1 J_4^{(a)} - J_5^{(a)}$). Hence, we are able to construct two more stored-energy functions which satisfy the stress-free reference configuration a priori, i.e.

$$\begin{aligned}
\psi_{(\mathrm{P2})}^{\mathrm{ti},(a)} &= \begin{cases} \frac{\alpha_3}{2\alpha_4}\{\exp[\alpha_4(K_1^{(a)}-1)^2]-1\} & \text{for } K_1^{(a)} \geqslant 1, \\ 0 & \text{for } K_1^{(a)} < 1, \end{cases} \\
\psi_{(\mathrm{P3})}^{\mathrm{ti},(a)} &= \begin{cases} \alpha_5 (K_1^{(a)}-1)^{\alpha_6} & \text{for } K_1^{(a)} \geqslant 1, \\ 0 & \text{for } K_1^{(a)} < 1, \end{cases}
\end{aligned} \tag{4.24}$$

with $\alpha_3 \geqslant 0$, $\alpha_4 > 0$, $\alpha_5 \geqslant 0$ and $\alpha_6 > 1$. The first one ($\psi_{(\mathrm{P2})}^{\mathrm{ti},(a)}$) represents a slight modification of the model of Holzapfel et al. while the second one characterizes the substitution of $J_4^{(a)}$ by $K_1^{(a)}$ in (4.21). The proof of polyconvexity for (4.24) is straightforward, since a convex and monotonically increasing function of a polyconvex argument is also polyconvex (Schröder and Neff, 2003), cf. Appendix A. After a short algebraic transformation we obtain $K_1^{(a)} = \|\mathrm{Cof}[\boldsymbol{F}]\boldsymbol{a}_{(a)}\|^2$ and see that $K_1^{(a)}$ controls the change of area with a unit normal into the preferred direction.

In Fig. 1 the values of J_4, K_1, K_2 and K_3 are illustrated for an uniaxial tension test of an incompressible material with preferred direction oriented parallelly to the stretch direction. We see, that for incompressible materials J_4 and K_3 increase when the material is elongated in the direction $\boldsymbol{a}_{(a)}$, and K_1 and K_2 increase if the material is shortened. Therefore, any function containing K_1 or K_2 proposed in this section (e.g., the function (4.24)) generates stresses only when the material is shortened in the preferred direction, which is physically not meaningful since collagen fibers mainly support tensile stresses. Nevertheless, it might be useful for some cases to activate stresses under such condition; then (4.24) may be utilized. Replacing $K_1^{(a)}$ in (4.24) by one of the polyconvex functions given in Schröder and Neff (2003)$_{(3.48)}$, viz.,

$$(K_1^{(a)})^2, \quad (K_1^{(a)})^3, \quad \frac{K_1^{(a)}}{I_3^{1/3}}, \quad \frac{(K_1^{(a)})^2}{I_3^{2/3}}, \tag{4.25}$$

would provide further polyconvex functions, but their physical interpretation for soft biological tissues may be difficult.

Two other polyconvex stored-energy functions are constructed by considering $K_3^{(a)}$. Due to the fact that $K_3^{(a)} = 2$ in the reference configuration, and in order to still satisfy the natural state condition a priori we introduce

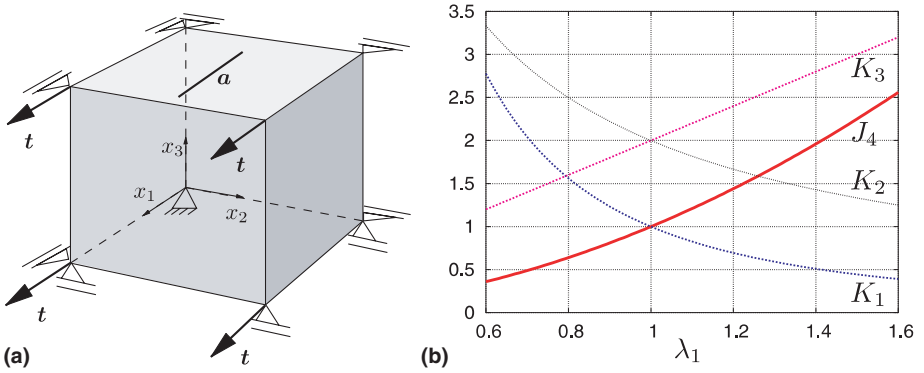

Fig. 1. (a) Uniaxial unconstrained tension of an incompressible material with preferred direction oriented parallelly to the stretch direction and (b) associated values of individual polyconvex functions J_4, K_1, K_2 and K_3 vs. stretch $\lambda_1 = (l_0 + \Delta l)/l_0$; l_0 is the cube length in 1-direction in the reference configuration and Δl denotes the difference between actual and reference length.

$$\psi^{\mathrm{ti},(a)}_{(\mathrm{P4})} = \begin{cases} \frac{\alpha_7}{2\alpha_8}\{\exp[\alpha_8(K_3^{(a)}-2)^2]-1\} & \text{for } K_3^{(a)} \geqslant 2, \\ 0 & \text{for } K_3^{(a)} < 2, \end{cases}$$
$$\psi^{\mathrm{ti},(a)}_{(\mathrm{P5})} = \begin{cases} \alpha_9(K_3^{(a)}-2)^{\alpha_{10}} & \text{for } K_3^{(a)} \geqslant 2, \\ 0 & \text{for } K_3^{(a)} < 2 \end{cases} \tag{4.26}$$

with $\alpha_7 \geqslant 0$, $\alpha_8 > 0$, $\alpha_9 \geqslant 0$ and $\alpha_{10} > 1$. These functions are also polyconvex, the proof of which is analogous to (4.24). Generally, the values of $K_3^{(a)}$ increase when the material is elongated in the preferred direction, see Fig. 1. Thus, (4.26) seem to be useful functions for soft biological tissues.

Other suitable polyconvex stored-energy functions, which also satisfy the stress-free reference configuration may be constructed by including the polyconvex functions found in Schröder and Neff (2003)$_{(3.53)}$, namely

$$(K_3^{(a)})^2, \quad \frac{K_3^{(a)}}{I_3^{1/3}}, \quad \frac{(K_3^{(a)})^2}{I_3^{1/3}}, \tag{4.27}$$

into (4.26). Then we obtain, for example,

$$\psi^{\mathrm{ti},(a)}_{(\mathrm{P6})} = \begin{cases} \frac{\alpha_{11}}{2\alpha_{12}}\{\exp[\alpha_{12}((K_3^{(a)})^2-4)^2]-1\} & \text{for } K_3^{(a)} \geqslant 2, \\ 0 & \text{for } K_3^{(a)} < 2, \end{cases}$$
$$\psi^{\mathrm{ti},(a)}_{(\mathrm{P7})} = \begin{cases} \alpha_{13}((K_3^{(a)})^2-4)^{\alpha_{14}} & \text{for } K_3^{(a)} \geqslant 2, \\ 0 & \text{for } K_3^{(a)} < 2, \end{cases}$$
$$\psi^{\mathrm{ti},(a)}_{(\mathrm{P8})} = \begin{cases} \frac{\alpha_{15}}{2\alpha_{16}}\left\{\exp\left[\alpha_{16}\left(\frac{(K_3^{(a)})^2}{I_3^{1/3}}-4\right)^2\right]-1\right\} & \text{for } \frac{(K_3^{(a)})^2}{I_3^{1/3}} \geqslant 4, \\ 0 & \text{for } \frac{(K_3^{(a)})^2}{I_3^{1/3}} < 4, \end{cases}$$
$$\psi^{\mathrm{ti},(a)}_{(\mathrm{P9})} = \begin{cases} \alpha_{17}\left(\frac{(K_3^{(a)})^2}{I_3^{1/3}}-4\right)^{\alpha_{18}} & \text{for } \frac{(K_3^{(a)})^2}{I_3^{1/3}} \geqslant 4, \\ 0 & \text{for } \frac{(K_3^{(a)})^2}{I_3^{1/3}} < 4 \end{cases} \tag{4.28}$$

with $\alpha_{11} \geqslant 0$, $\alpha_{12} > 0$, $\alpha_{13} \geqslant 0$, $\alpha_{14} > 1$, $\alpha_{15} \geqslant 0$, $\alpha_{16} > 0$, $\alpha_{17} \geqslant 0$ and $\alpha_{18} > 1$; recall that $K_1^{(a)} = J_5^{(a)} - I_1 J_4^{(a)} + I_2$ and $K_3^{(a)} = I_1 J_4^{(a)} - J_5^{(a)}$.

It is worth noting that each other monotonically increasing function, e.g., also $\cosh(\cdots)$, etc., with positive and polyconvex arguments would lead to a polyconvex function, too. As an example, if the function proposed by Rüter and Stein (2000) is embedded into the case distinction, i.e.

$$\psi_{(\mathrm{P10})}^{\mathrm{ti},(a)} = \begin{cases} \alpha_{19}[\cosh(J_4^{(a)} - 1) - 1] & \text{for } J_4^{(a)} \geqslant 1, \\ 0 & \text{for } J_4^{(a)} < 1, \end{cases} \tag{4.29}$$

then this would be a polyconvex function. Of course, other polyconvex functions could be obtained by replacing $J_4^{(a)}$ with any other polyconvex function, as, e.g., (4.22), (4.23), (4.25), (4.27), provided that the case distinction is adopted accordingly.

5. Adjustment for soft biological tissues

5.1. Experimental data of a human aortic layer

In order to give an example of handling the polyconvex functions provided in the last sections we adjust some of these functions to a biological material. As an example, we consider an abdominal aorta from a human cadaver (male, 40 years, primary disease: congestive cardiomyopathy), which has been excised during autopsy within 24 h after death. The arterial wall was separated anatomically into the three layers, i.e. intima, media and adventitia. In the present work we focus on the media (i.e. the middle layer of the artery), which consists of smooth muscle cells, collagenous fibers, elastin in form of fenestrated elastic lamellae, and ground substance. The structured arrangement of these constituents gives the media high strength, resilience and the ability to resist loads in both the longitudinal and circumferential directions. Note that from the mechanical perspective, the media is the most significant layer in a healthy artery. Hence, more detailed investigations of medial layers may better explain their function on the basis of their structure and mechanics, i.e. vital information for clinical treatments of artery diseases.

From the media, strip samples with axial and circumferential orientations were cut out so that two specimens were obtained, as illustrated in Fig. 2 (for representative tissue samples see, for example, Fig. 4 in Holzapfel et al., 2004b). Prior to testing, pre-conditioning was achieved by executing five loading and unloading cycles at a constant crosshead speed of 1 mm/min for each test to obtain repeatable stress–strain curves. Subsequently, the strips underwent uniaxial extension tests (loading and unloading) in 0.9% NaCl solution at 37 °C with continuous recording of tensile force, strip width and gage length at a constant crosshead speed of 1 mm/min. For details on the customized tensile testing machine the reader is referred to Schulze-Bauer et al. (2002). The results of the experiment for the tension in circumferential and longitudinal direction are illustrated in Fig. 2. Additional experimental data for uniaxial extension tests for the Intima and Adventitia are given in Holzapfel (in press).

5.2. Representation of the arterial tissue

The non-collagenous matrix of the media is treated as an isotropic material, while the embedded collagen fibers, which appear as two families arranged in symmetrical spirals, are treated by the proposed anisotropic contributions, in particular by two superposed energies for the two fiber families ($n = 2$).

For the description of the stress–strain response, as illustrated in Fig. 2, we compare three polyconvex models. The first one is the model of Holzapfel et al. (2000, 2004a), which is given by the polyconvex isotropic part (4.17) and the convex transversely isotropic part (4.20). In the present work we incorporate the

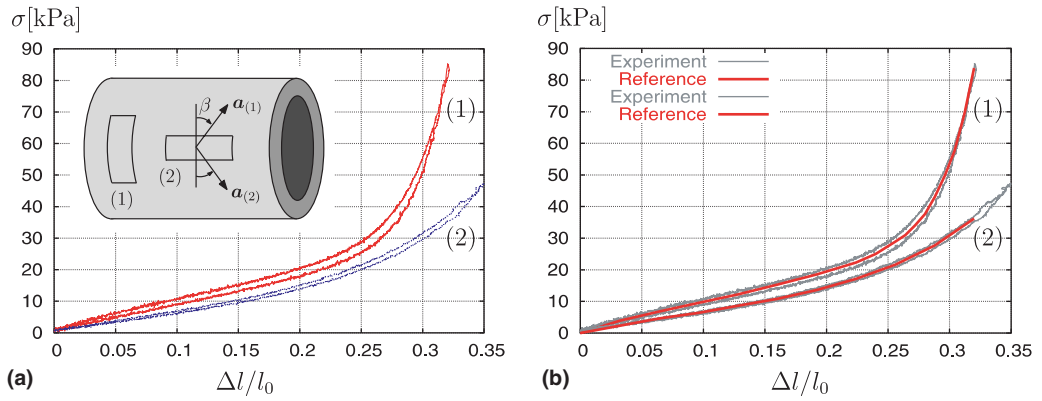

Fig. 2. Cauchy stress σ (kPa) vs. strain $\Delta l/l_0$ of the (a) experimental tension tests (loading and unloading) of a circumferentially (1) and longitudinally (2) oriented strip extracted from the media of a human abdominal aorta and (b) the considered associated reference curves. l_0 is the reference length of the strips while Δl is denoting the difference between actual and reference length.

Table 1
Material parameters of the model of Holzapfel et al. (2000)

$c_1 = \mu/2$ (kPa)	k_1 (kPa)	k_2
10.2069	0.00170	882.847

The angle between the (mean) fiber direction and the circumferential direction in the media was predicted to be 43.39°. The fiber angle acts here as a phenomenological parameter.

quasi-incompressibility through a special finite element approach. The material parameters for the best fit to the experimental data are shown in Table 1.

For the response of the constitutive model of Holzapfel et al. see Fig. 3. Therein the Cauchy stresses are depicted for the circumferentially and longitudinally oriented strips. As can be seen, the match is quite good, even though the strong exponential character is underestimated. The (exponential) stiffening effect at higher loads may be described with higher accuracy by introducing one additional dimensionless parameter ranging between zero and one, as recently proposed in Holzapfel et al. (2004c, in press). The additional parameter is then a measure of anisotropy. For zero the function reduces to an isotropic (rubber-like) model, similar to that proposed in Demiray (1972), while for one the function reduces to the model proposed in Holzapfel et al. (2000).

In order to analyze the accuracy of the matching of the experimental data by the model more precisely the following relative error

$$r := \frac{|\sigma^{\exp} - \sigma^{\mathrm{mod}}|}{|\sigma^{\exp}_{\max}|} \tag{5.30}$$

is introduced. Herein, $\sigma^{\exp}$ and σ^{mod} denote the experimental stresses (as illustrated in Fig. 2b as the solid lines) and the stresses computed by the constitutive model, respectively. Note that r should be as low as possible and would become zero for a perfect matching. The benchmark of the adjustment for a complete experiment can be accomplished by the definition of the quantity

$$\bar{r} := \frac{1}{|\sigma^{\exp}_{\max}|}\sqrt{\frac{1}{n}\sum\nolimits_{i=1}^{n}(\sigma_i^{\exp} - \sigma_i^{\mathrm{mod}})^2}, \tag{5.31}$$

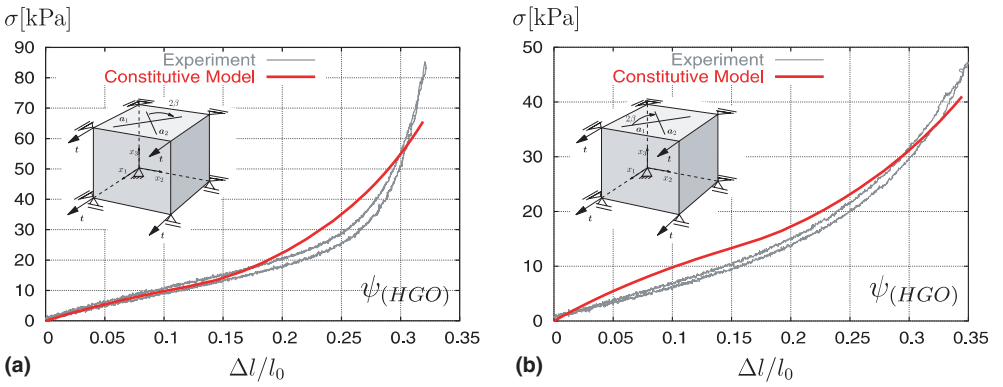

Fig. 3. Cauchy stress σ (kPa) vs. strain $\Delta l/l_0$ of the experiment and the constitutive model of Holzapfel et al. (2000): (a) circumferentially and (b) longitudinally oriented strips. l_0 is the reference length of the strip and Δl the change of length.

wherein the total number of the experimental data-points i is denoted by n. In Fig. 4 the relative error is shown for the two experiments and for the circumferentially oriented strip we obtain $\bar{r} = 0.081$ and for the longitudinally oriented strip we receive $\bar{r} = 0.064$.

In the present paper we are concerned with the easy fitting of polyconvex stored energies to soft tissues. For an example, we consider another polyconvex function, whose parameters can easily be adjusted. Therefore, we do not use any optimization procedure for the adjustment here and obtain the material parameters by 'hand-fitting'. For the second polyconvex model we keep the isotropic part of the Holzapfel, Gasser and Ogden-model and add the function (4.19) in order to consider the quasi-incompressibility constraint via a penalty function. Then the isotropic part of the stored energy reads

$$\psi^{\text{iso}}_{(1)} = c_1\left(\frac{I_1}{I_3^{1/3}} - 3\right) + \varepsilon\left(I_3^{\gamma} + \frac{1}{I_3^{\gamma}} - 2\right), \quad c_1 > 0, \;\; \varepsilon > 0, \;\; \gamma > 1. \tag{5.32}$$

The coercivity issue for this isotropic energy has been investigated in Hartmann and Neff (2003). For the description of the material behavior in fiber direction we account for the transversely isotropic part given in (4.21) and we obtain the complete anisotropic part

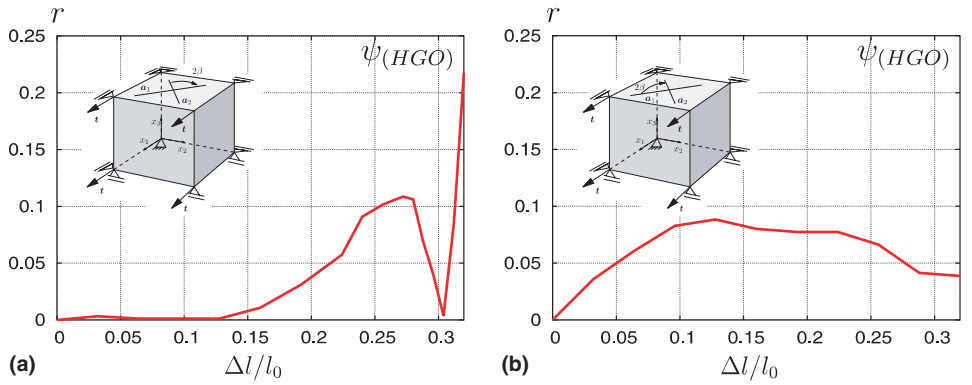

Fig. 4. Relative error r vs. strain $\Delta l/l_0$ using the constitutive model of Holzapfel et al. (2000): (a) circumferentially ($\bar{r} = 0.081$) and (b) longitudinally oriented strips ($\bar{r} = 0.064$).

$$\psi_{(1)}^{\text{aniso}} = \begin{cases} \sum_{a=1}^{2}[\alpha_1(J_4^{(a)}-1)^{\alpha_2}] & \text{for } J_4^{(1)} \geqslant 1 \wedge J_4^{(2)} \geqslant 1, \\ \alpha_1(J_4^{(1)}-1)^{\alpha_2} & \text{for } J_4^{(1)} \geqslant 1 \wedge J_4^{(2)} < 1, \\ \alpha_1(J_4^{(2)}-1)^{\alpha_2} & \text{for } J_4^{(1)} < 1 \wedge J_4^{(2)} \geqslant 1, \\ 0 & \text{for } J_4^{(1)} < 1 \wedge J_4^{(2)} < 1. \end{cases} \tag{5.33}$$

In this model c_1 scales the isotropic stress response which is seen in the nearly linear behavior of the curve below $\Delta l/l_0 \approx 0.15$ in Fig. 2. The parameters ε and γ control the volumetric deformation; this is important in order to satisfy the quasi-incompressibility constraint. α_2 accounts for the level of curvature in fiber direction and α_1 scales this response.

The material parameters of the adjusted model $\psi_{(1)}$ are presented in Table 2 and the results are illustrated in Fig. 5. As can be seen the stress–strain response for the two experiments is represented quite accurately, even though the exponential character is also slightly underestimated.

In Fig. 6 the measure r is depicted and for the circumferentially and the longitudinally oriented strips we obtain $\bar{r} = 0.059$ and 0.037, respectively.

A drawback of the previous two models becomes obvious when the stress–strain response of the two experiments is depicted in the same diagram. One of the main characteristics of the experimental data is that the curves for the circumferentially and longitudinally oriented strip differ right from the beginning for these particular strips investigated. In Fig. 7 we see that the two models are not able to represent this behavior, because here, the curves start to differ at approximately $\Delta l/l_0 \approx 0.15$.

Table 2
Material parameters of the model $\psi_{(1)}$

c_1 (kPa)	ε (kPa)	γ	α_1 (kPa)	α_2
13.5	10.0	20.0	10^{14}	20.0

The angle between the (mean) fiber direction and the circumferential direction in the media was predicted to be 43.39°. The fiber angle acts here as a phenomenological parameter.

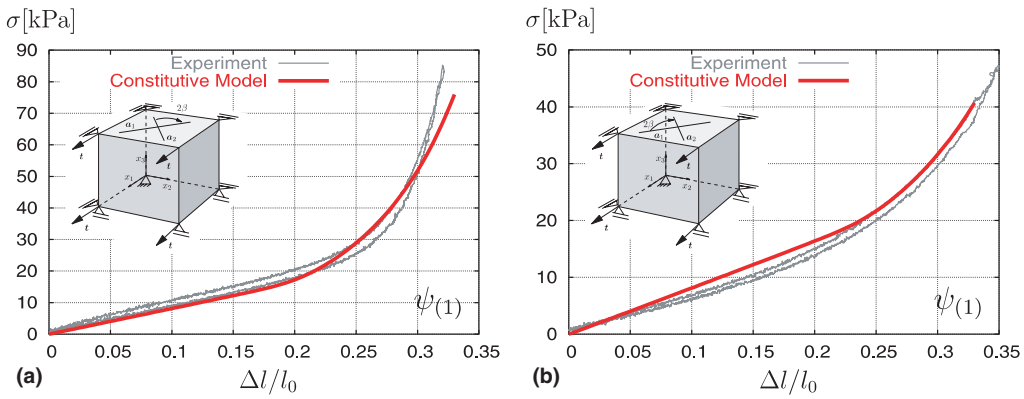

Fig. 5. Cauchy stress σ (kPa) vs. strain $\Delta l/l_0$ of the experiment and the constitutive model $\psi_{(1)}$: (a) circumferentially and (b) longitudinally oriented strips.

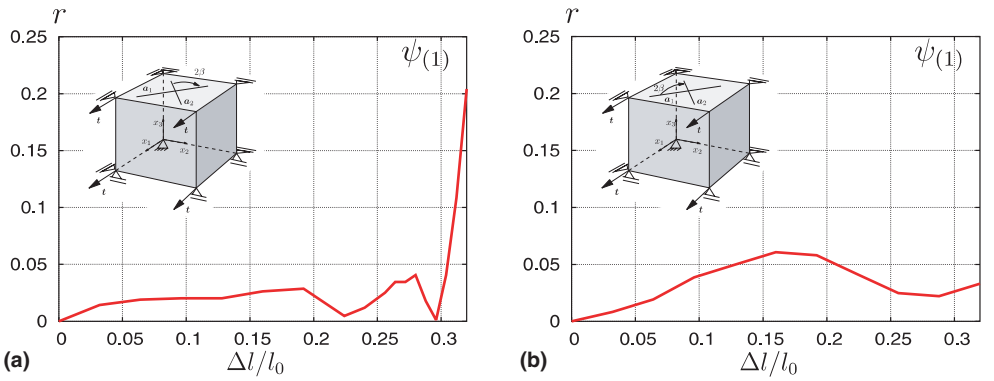

Fig. 6. Relative error r vs. strain $\Delta l/l_0$ using the constitutive model $\psi_{(1)}$: (a) circumferentially ($\bar{r} = 0.059$) and (b) longitudinally oriented strips ($\bar{r} = 0.037$).

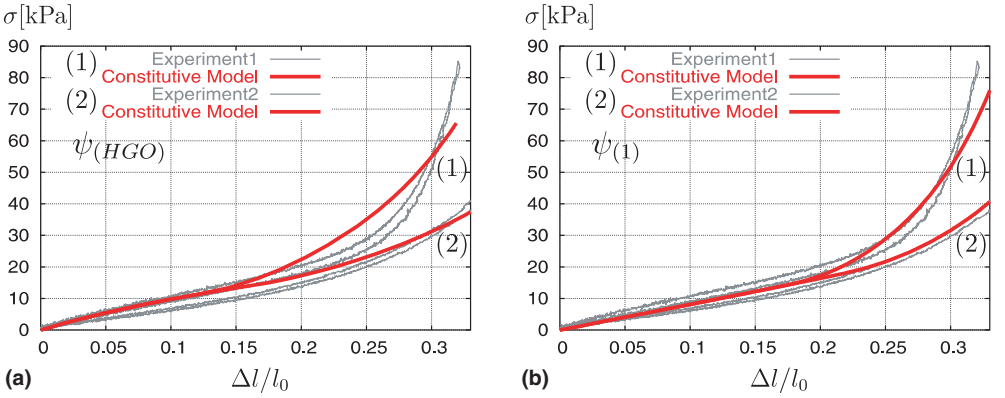

Fig. 7. Cauchy stress σ (kPa) vs. strain $\Delta l/l_0$ of the two experiments and the constitutive models (a) $\psi_{(\mathrm{HGO})}$ and (b) $\psi_{(1)}$.

In order to overcome this deviation we additionally consider the transversely isotropic function given in $(4.26)_2$, and we obtain for two fiber families the case distinction

$$\psi_{(2)}^{\mathrm{aniso}} = \begin{cases} \sum_{a=1}^{2} [\alpha_3 (K_3^{(a)} - 2)^{\alpha_4}] & \text{for } K_3^{(1)} \geqslant 2 \wedge K_3^{(2)} \geqslant 2, \\ \alpha_3 (K_3^{(1)} - 2)^{\alpha_4} & \text{for } K_3^{(1)} \geqslant 2 \wedge K_3^{(2)} < 2, \\ \alpha_3 (K_3^{(2)} - 2)^{\alpha_4} & \text{for } K_3^{(1)} < 2 \wedge K_3^{(2)} \geqslant 2, \\ 0 & \text{for } K_3^{(1)} < 2 \wedge K_3^{(2)} < 2. \end{cases} \tag{5.34}$$

Then the polyconvex model for the description of the medial layer of a human abdominal aorta reads

$$\psi_{(2)} = \psi_{(1)}^{\mathrm{iso}} + \psi_{(1)}^{\mathrm{aniso}} + \psi_{(2)}^{\mathrm{aniso}}. \tag{5.35}$$

As before, $\psi_{(1)}^{\mathrm{aniso}}$ describes the exponential-type behavior in the fiber direction, while $\psi_{(2)}^{\mathrm{aniso}}$ takes care of the different curves for the circumferentially and longitudinally oriented strips in the low load domain. In order to show the easy handling the model is adjusted to the experimental data by 'hand-fitting'. The chosen parameters are summarized in Table 3.

Table 3
Material parameters of the model $\psi_{(2)}$

c_1 (kPa)	ε (kPa)	γ	α_1 (kPa)	α_2	α_3 (kPa)	α_4
8.5	22.0	10.8	9×10^{14}	20.5	17.0	1.8

The angle between the (mean) fiber direction and the circumferential direction in the media was predicted to be 43.39°. The fiber angle acts here as a phenomenological parameter.

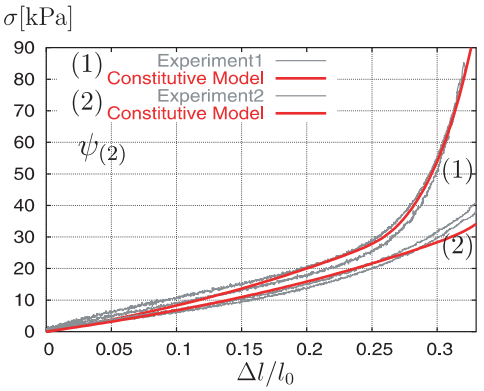

Fig. 8. Cauchy stress σ (kPa) vs. strain $\Delta l/l_0$ of the experiment ((1) circumferentially and (2) longitudinally oriented strip). The fit is based on the constitutive model $\psi_{(2)}$.

In Fig. 8 the response of the model $\psi_{(2)}$ is compared to the experimental data. First, we see that the exponential character of the stress–strain behavior of the considered tissue is no longer underestimated and the curve for the circumferentially oriented strip fits the experimental data very well. Secondly, ab initio the deviating curves for the circumferentially and longitudinally oriented strips, as seen in the experiment, may be described accurately. Only the curve (2) underestimates the stress response slightly for $\Delta l/l_0 > 0.27$.

For the objective analysis of the adjustment accuracy the quantity r is depicted in Fig. 9 and for the circumferentially and longitudinally oriented strip we obtain $\bar{r} = 0.017$ and 0.044, respectively.

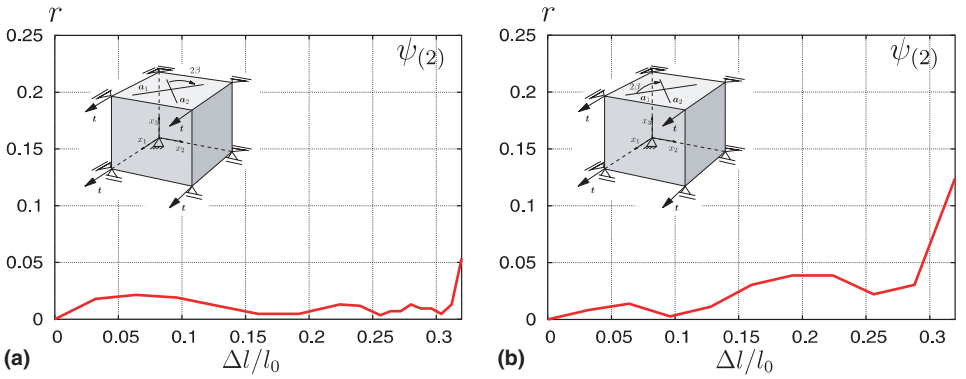

Fig. 9. Relative error r vs. strain $\Delta l/l_0$ using the constitutive model $\psi_{(2)}$: (a) circumferentially ($\bar{r} = 0.017$) and (b) longitudinally oriented strips ($\bar{r} = 0.044$).

Hereby, it is shown that polyconvex stored-energy functions can be utilized generally for the representation of soft biological tissues and its adjustment can be done in an easy way.

6. Conclusion

In this paper, we focussed on the construction of new polyconvex stored energies, which were able to represent the characteristic material behavior of a particular soft biological tissue. Another main focus has been on the simplicity of the proposed energies in order to obtain a set of polyconvex functions that are easy to handle. The novel approach in this context was the formulation of a construction principle for polyconvex functions which additionally satisfy the stress-free reference condition a priori. Then a variety of polyconvex functions has been proposed by means of the defined principle. The medial layer of one human abdominal aorta has been extracted and analyzed as a representative collagenous soft biological tissue. Herein, two test stripes were cut out and its stress–strain response was investigated. Then some of the proposed polyconvex functions were 'hand-fitted' to the experimental data and compared to a frequently used model for soft tissues. Some remarks were given as to the way the functions may be chosen and how the material parameters control the stress–strain response.

Appendix A. Proof of convexity

Convexity of (4.20). Neglecting the constant terms in (4.20), which do not contribute to the derivatives of the energy, we show that for any $p > 2$

$$W^{\mathrm{ti}}(\boldsymbol{F}) = \begin{cases} \exp(\|\boldsymbol{Fa}\|^2 - 1)^p & \text{for } \|\boldsymbol{Fa}\|^2 \geqslant 1, \\ 0 & \text{for } \|\boldsymbol{Fa}\|^2 < 1 \end{cases}$$

is convex with respect to $\boldsymbol{F}$. For this purpose, we compute the piecewise second differential.

Since

$$D_F[\exp(\|\boldsymbol{Fa}\|^2 - 1)^p].\boldsymbol{H} = \exp(\|\boldsymbol{Fa}\|^2 - 1)^p \left[p\Big(\|\boldsymbol{Fa}\|^2 - 1 \Big)^{p-1} 2\langle \boldsymbol{Fa}, \boldsymbol{Ha} \rangle \right],$$

we obtain for the non-zero branch of W^{ti}

$$\begin{aligned} D_F^2 W^{\mathrm{ti}}(\boldsymbol{F}).(\boldsymbol{H},\boldsymbol{H}) = {} & \exp(\|\boldsymbol{Fa}\|^2 - 1)^p [p(\|\boldsymbol{Fa}\|^2 - 1)^{p-1} 2\langle \boldsymbol{Fa}, \boldsymbol{Ha} \rangle]^2 \\ & + \exp(\|\boldsymbol{Fa}\|^2 - 1)^p 2p[(p-1)(\|\boldsymbol{Fa}\|^2 - 1)^{p-2} 2\langle \boldsymbol{Fa}, \boldsymbol{Ha} \rangle^2 + (\|\boldsymbol{Fa}\|^2 - 1)^{p-1} \langle \boldsymbol{Ha}, \boldsymbol{Ha} \rangle]. \end{aligned}$$

This formula tends continuously to zero for $\|\boldsymbol{Fa}\|^2 \to 1$ and is positive for $\|\boldsymbol{Fa}\|^2 \geqslant 1$. Hence, the complete second differential is always positive and continuous. By continuity, we obtain that W^{ti} is convex for $p = 2$, too. Furthermore, convexity of W^{ti} implies Legendre–Hadamard ellipticity. It is clear that any additive composition of W^{ti} with an isotropic elliptic energy will also remain Legendre–Hadamard elliptic.

Convexity of (4.21). For proving convexity of (4.21) we compute the piecewise second differential of the non-zero branch of (4.21), i.e. $W_1^{\mathrm{ti}}(\boldsymbol{F}) = (\|\boldsymbol{Fa}\|^2 - 1)^p$. Since

$$D_F[W_1^{\mathrm{ti}}].\boldsymbol{H} = p(\|\boldsymbol{Fa}\|^2 - 1)^{p-1} 2\langle \boldsymbol{Fa}, \boldsymbol{Ha} \rangle$$

we obtain

$$D_F^2[W_1^{\mathrm{ti}}].(\boldsymbol{H},\boldsymbol{H}) = 2p[(p-1)(\|\boldsymbol{Fa}\|^2 - 1)^{p-2} 2\langle \boldsymbol{Fa}, \boldsymbol{Ha} \rangle^2 + (\|\boldsymbol{Fa}\|^2 - 1)^{p-1} \langle \boldsymbol{Ha}, \boldsymbol{Ha} \rangle].$$

For $\|\boldsymbol{Fa}\|^2 \to 1$ the second differential tends to zero and is positive for $\|\boldsymbol{Fa}\|^2 > 1$ and each $p \geqslant 1$, thus, the function is convex with respect to $\boldsymbol{F}$ and therefore Legendre–Hadamard-elliptic.

Polyconvexity of (4.24)$_1$, (4.26)$_1$, (4.28)$_1$ and (4.28)$_3$. For the proof of polyconvexity we show that for any $p > 2$ and constant c

$$W_2^{\mathrm{ti}}(K) = \begin{cases} \exp(K-c)^p & \text{for } K \geqslant c, \\ 0 & \text{for } K < c \end{cases} \tag{A.36}$$

is monotonically increasing and convex with respect to K (in general K will be a polyconvex function). For this purpose, we compute the first derivative of W_2^{ti}

$$\partial_K[W_2^{\mathrm{ti}}] = \exp[(K-c)^p][p(K-c)^{p-1}]$$

and see that W_2^{ti} is positive for $K \geqslant c$ and therefore altogether monotonically increasing. In order to show convexity we compute the second derivative of W_2^{ti}

$$\partial^2_{KK}[W_2^{\mathrm{ti}}] = \exp[(K-c)^p][p(K-c)^{p-1}]^2 + \exp[(K-c)^p]p(p-1)(K-c)^{p-2}.$$

This formula tends continuously to zero for $K \to c$ and is positive for $K \geqslant c$. Hence, the second derivative is always positive and continuous. By continuity, we obtain that W_2^{ti} is convex also for $p = 2$.

Polyconvexity of (4.24)$_2$, (4.26)$_2$, (4.28)$_2$ and (4.28)$_4$. For the proof of polyconvexity we show that for any $p > 1$ and constant c

$$W_3^{\mathrm{ti}}(K) = \begin{cases} (K-c)^p & \text{for } K \geqslant c, \\ 0 & \text{for } K < c \end{cases} \tag{A.37}$$

is monotonically increasing and convex with respect to K (in general K is a polyconvex function). For this purpose, we compute the first derivative of W_3^{ti}

$$\partial_K[W_3^{\mathrm{ti}}] = p(K-c)^{p-1}$$

and notice that W_3^{ti} is positive and therefore monotonically increasing for $K \geqslant c$. For showing convexity we compute the second derivative

$$\partial^2_{KK}[W_3^{\mathrm{ti}}] = p(p-1)(K-c)^{p-2}.$$

For $K \to c$ the second derivative tends to zero and is positive for $K > c$ and each $p > 1$, thus, the function is polyconvex, since K is polyconvex.

References

Almeida, E.S., Spilker, R.L., 1998. Finite element formulation for hyperelastic transversely isotropic biphasic soft tissues. Computer Methods in Applied Mechanics and Engineering 151, 513–538.

Ball, J.M., 1977a. Convexity conditions and existence theorems in non-linear elasticity. Archive of Rational Mechanics and Analysis 63, 337–403.

Ball, J.M., 1977b. Constitutive inequalities and existence theorems in nonlinear elastostatics. In: Knops, R.J. (Ed.), Nonlinear Analysis and Mechanics, á Heriot-Watt Symposium, vol. 1. Pitman.

Ball, J.M., James, R.D., 1992. Proposed experimental tests of a theory of fine microstructure and the two well problem. Philosophical Transactions of Royal Society of London 338, 389–450.

Betten, J., 1987. Formulation of anisotropic constitutive equations. In: Boehler, J.P. (Ed.), Applications of Tensor Functions in Solid Mechanics, CISM Course No. 292. Springer-Verlag.

Boehler, J.P., 1987. Introduction to the invariant formulation of anisotropic constitutive equations. In: Boehler, J.P. (Ed.), Applications of Tensor Functions in Solid Mechanics, CISM Course No. 292. Springer-Verlag.

Ciarlet, P.G., 1988. Mathematical Elasticity, vol. 1: Three Dimensional Elasticity. Elsevier Science Publishers, North-Holland.

Dacorogna, B., 1989. Direct methods in the calculus of variations. Applied Mathematical Science, vol. 78. Springer-Verlag.

Demiray, H., 1972. A note on the elasticity of soft biological tissues. Journal of Biomechanical Engineering 5, 309–311.
Fung, Y.C., Fronek, K., Patitucci, P., 1979. Pseudoelasticity of arteries and the choice of its mathematical expression. American Physiological Society 237, H620–H631.
Gasser, T.C., Holzapfel, G.A., 2002. A rate-independent elastoplastic constitutive model for (biological) fiber–reinforced composites at finite strains: continuum basis, algorithmic formulation and finite element implementation. Computational Mechanics 29, 340–360.
Gurevich, G.B., 1964. Foundations of the Theory of Algebraic Invariants, Noordhoff (English translation).
Hartmann, S., Neff, P., 2003. Existence theory for a modified polyconvex hyperelastic relation of generalized polynomial-type in the case of nearly-incompressibility. International Journal of Solid and Structures 40, 2767–2791.
Holzapfel, G.A., in press. Determination of material models for arterial walls from uniaxial extension tests and histological structure. Journal of Theoretical Biology.
Holzapfel, G.A., Gasser, Th.C., Ogden, R.W., 2000. A new constitutive framework for arterial wall mechanics and a comparative study of material models. Journal of Elasticity 61, 1–48.
Holzapfel, G.A., Gasser, T.C., Stadler, M., 2002. A structural model for the viscoelastic behavior of arterial walls: continuum formulation and finite element analysis. European Journal of Mechanics—A/Solids 21, 441–463.
Holzapfel, G.A., Gasser, Th.C., Ogden, R.W., 2004a. Comparison of a multi-layer structural model for arterial walls with a fung-type model, and issues of material stability. ASME Journal of Biomechanical Engineering 126, 264–275.
Holzapfel, G.A., Sommer, G., Regitnig, P., 2004b. Anisotropic mechanical properties of tissue components in human atherosclerotic plaques. Journal of Biomechanical Engineering 126, 657–665.
Holzapfel, G.A., Stadler, M., Gasser, T.C., 2004c. Changes in the mechanical environment of stenotic arteries during interaction with stents: computational assessment of parametric stent design. Journal of Biomechanical Engineering 127, 166–180.
Holzapfel, G.A., Sommer, G., Gasser, C.T., Regitnig, P., in press. Determination of the layer-specific mechanical properties of human coronary arteries with non-atherosclerotic intimal thickening, and related constitutive modelling. American Journal of Physiology: Heart and Circulatory Physiology.
Humphrey, J.D., 2002. Cardiovascular Solid Mechanics. Cells, Tissues and Organs. Springer-Verlag, New York.
Itskov, M., Aksel, N., 2004. A class of orthotropic and transversely isotropic hyperelastic constitutive models based on a polyconvex strain energy function. International Journal of Solids and Structures 41, 3833–3848.
Krawietz, A., 1986. Materialtheorie—Mathematische Beschreibung des phänomenologischen thermomechanischen Verhaltens. Springer-Verlag.
Marsden, J.E., Hughes, J.R., 1983. Mathematical Foundations of Elasticity. Prentice-Hall.
Merodio, J., Neff, P., submitted for publication. A note on tensile instabilities and loss of ellipticity for a fiber–reinforced nonlinearly elastic solid.
Morrey, C.B., 1952. Quasi–convexity and the lower semicontinuity of multiple integrals. Pacific Journal of Mathematics 2, 25–53.
Müller, S., 1999. Variational models for microstructure and phase transitions. In: Calculus of Variations and Geometric Evolutions Problems. Lecture Notes in Mathematics, vol. 1713, Springer, Berlin, pp. 85–210.
Roach, M.R., Burton, A.C., 1957. The reason for the shape of the distensibility curve of arteries. Canadian Journal of Biochemistry and Physiology 35, 681–690.
Rüter, M., Stein, E., 2000. Analysis, finite element computation and error estimation in transversely isotropic nearly incompressible finite elasticity. Computer Methods in Applied Mechanics and Engineering 190, 519–541.
Schröder, J., Neff, P., 2001. On the construction of polyconvex anisotropic free energy functions. In: Miehe, C. (Ed.), Proceedings of the IUTAM Symposium on Computational Mechanics of Solid Materials at Large Strains. Kluwer Academic Publishers, Dordrecht, pp. 171–180.
Schröder, J., Neff, P., 2003. Invariant formulation of hyperelastic transverse isotropy based on polyconvex free energy functions. International Journal of Solids and Structures 40, 401–445.
Schröder, J., Neff, P., Balzani, D., 2004. A variational approach for materially stable anisotropic hyperelasticity. International Journal of Solids and Structures 42 (15), 4352–4371.
Schulze-Bauer, C.A.J., Regitnig, P., Holzapfel, G.A., 2002. Mechanics of the human femoral adventitia including high-pressure response. American Journal of Physiology: Heart and Circulatory Physiology 282, H2427–H2440.
Silhavý, M., 1997. The Mechanics and Thermodynamics of Continuous Media. Springer-Verlag.
Spencer, A.J.M., 1971. Theory of invariants. In: Eringen, A.C. (Ed.), Continuum Physics, vol. 1. Academic Press, New York, pp. 239–353.
Spencer, A.J.M., 1987. Isotropic polynomial invariants and tensor functions. In: Boehler, J.P. (Ed.), Applications of Tensor Functions in Solid Mechanics, CISM Course No. 282. Springer-Verlag.
Steigmann, D.J., 2003. Frame-invariant polyconvex strain-energy functions for some anisotropic solids. Mathematics and Mechanics of Solids 8, 497–506.
Truesdell, C., Noll, W., 2004. In: Antman, S.S. (Ed.), The Non-Linear Field Theories of Mechanics, third ed. Springer-Verlag, Berlin.
Weiss, J.A., Maker, B.N., Govindjee, S., 1996. Finite element implementation of incompressible, transversely isotropic hyperelasticity. Computer Methods in Applied Mechanics and Engineering 135, 107–128.

Zheng, Q.S., Spencer, A.J.M., 1993a. On the canonical representations for Kronecker powers of orthogonal tensors with application to material symmetry problems. International Journal of Engineering Science 31 (4), 617–635.
Zheng, Q.S., Spencer, A.J.M., 1993b. Tensors which characterize anisotropies. International Journal of Engineering Science 31 (5), 679–693.
Zheng, Q.S., Boehler, J.P., 1994. The description, classification, and reality of material and physical symmetries. Acta Mechanica 102, 73–89.